

1 **Uncovering the gastrointestinal passage, intestinal epithelial cellular uptake and Ago2 loading of**
2 **milk miRNAs in neonates using xenobiotic tracers**

3 Patrick Philipp Weil¹, Susanna Reincke¹, Christian Alexander Hirsch¹, Federica Giachero¹, Malik
4 Aydin^{1,2}, Jonas Scholz³, Franziska Jönsson³, Claudia Hagedorn³, Duc Ninh Nguyen⁴, Thomas
5 Thymann⁴, Anton Pembaur¹, Valerie Orth⁵, Victoria Wünsche¹, Ping-Ping Jiang^{4,6} Stefan Wirth²,
6 Andreas C. W. Jenke⁷, Per Torp Sangild⁴, Florian Kreppel³, Jan Postberg^{1,*}

7 *corresponding author

8

9 **Authors and e-mail addresses:**

10 Patrick Philipp Weil patrick.weil@uni-wh.de
11 Susanna Reincke susanna.reincke@uni-wh.de
12 Christian Alexander Hirsch christian.hirsch@uni-wh.de
13 Federica Giachero federica.giachero@uni-wh.de
14 Malik Aydin malik.aydin@uni-wh.de
15 Jonas Scholz jonas.scholz@uni-wh.de
16 Franziska Jönsson franziska.joensson@uni-wh.de
17 Claudia Hagedorn claudia.hagedorn@uni-wh.de
18 Duc Ninh Nguyen dnn@sund.ku.dk
19 Thomas Thymann thomas.thymann@sund.ku.dk
20 Ping-Ping Jiang jiangpp3@mail.sysu.edu.cn
21 Anton Pembaur anton.pembaur@uni-wh.de
22 Valerie Orth valerie.orth@helios-gesundheit.de
23 Victoria Wünsche victoria.wuensche@uni-wh.de
24 Stefan Wirth stefan.wirth@helios-gesundheit.de
25 Andreas C. W. Jenke andreas.jenke@klinikum-kassel.de
26 Per Torp Sangild pts@sund.ku.dk
27 Florian Kreppel florian.kreppel@uni-wh.de
28 Jan Postberg jan.postberg@uni-wh.de

29 ¹Clinical Molecular Genetics and Epigenetics, Faculty of Health, Centre for Biomedical Education &
30 Research (ZBAF), Witten/Herdecke University, Alfred-Herrhausen-Str. 50, 58448 Witten, Germany

31 ²HELIOS University Hospital Wuppertal, Children's Hospital, Centre for Clinical & Translational
32 Research (CCTR), Witten/Herdecke University, Heusnerstr. 40, 42283 Wuppertal, Germany

33 ³Chair of Biochemistry and Molecular Medicine, Faculty of Health, Centre for Biomedical Education
34 and Research (ZBAF), Witten/Herdecke University, Stockumer Str. 10, 58453 Witten, Germany

35 ⁴Comparative Pediatrics and Nutrition, Department of Veterinary and Animal Sciences, University of
36 Copenhagen, Copenhagen, Denmark

37 ⁵HELIOS University Hospital Wuppertal, Department of Surgery II, Centre for Clinical &
38 Translational Research (CCTR), Witten/Herdecke University, Heusnerstr. 40, 42283 Wuppertal,
39 Germany

40 ⁶School of Public Health, Sun Yat-sen University, Guangzhou, China

41 ⁷Klinikum Kassel, Zentrum für Kinder- und Jugendmedizin, Neonatologie und allgemeine Pädiatrie,
42 Mönchebergstr. 41-43, 34125 Kassel, Germany

43

44 **Preprint**

45 medRxiv.org: doi: <https://doi.org/10.1101/2021.08.24.21262525>

46

47 **Abbreviations**

48 Adenovirus-type 5 (Ad5); gastrointestinal passage (GI passage); human intestinal epithelial cells
49 (HIEC); necrotizing enterocolitis (NEC); post-transcriptional gene silencing (PTGS); RNA
50 interference (RNAi); transcriptional gene silencing (TGS)

51

52 **Short title**

53 Milk miRNA GI passage and intestinal cellular uptake

54 **Abstract**

55 **Background:** Exclusive breastfeeding is the best source of nutrition for most infants, but it is not
56 always possible. Enteral nutrition influences intestinal gene regulation and the susceptibility for
57 inflammatory bowel disorders, such as necrotizing enterocolitis (NEC). In modern neonatology it is
58 observed that lactase activity increases during intestinal maturation, but formula-fed infants exhibit
59 lower activity levels than milk-fed infants.

60 **Objective:** We interrogate the transmissibility of milk miRNAs, since human breast milk has a high
61 miRNA content in comparison to other body fluids. Our data contribute to the controversial discussion
62 whether milk miRNAs could influence gene regulation in term and preterm neonates and thus might
63 vertically transmit developmental relevant signals.

64 **Design:** Following their cross-species profiling via miRNA deep-sequencing we utilized dietary
65 xenobiotic taxon-specific milk miRNA as tracers in human and porcine neonates, followed by
66 functional studies in primary human fetal intestinal epithelial cells (HIEC-6) using Ad5-mediated
67 miRNA-gene transfer.

68 **Results:** We show that mammals have in common many milk miRNAs yet exhibit taxon-specific
69 miRNA fingerprints. We traced intact bovine-specific miRNAs from formula-nutrition in human
70 preterm stool and 9 days after the onset of enteral feeding in intestinal cells of preterm piglets. Few
71 hours after introducing enteral feeding in preterm piglets with supplemented reporter miRNAs (cel-
72 miR-39-5p/-3p), we observed enrichment of the xenobiotic cel-miR in blood serum and in Ago2-
73 immunocomplexes from intestinal biopsies. In contrast, we did not observe xenobiotic miRNAs in
74 neonatal porcine cerebrospinal fluid.

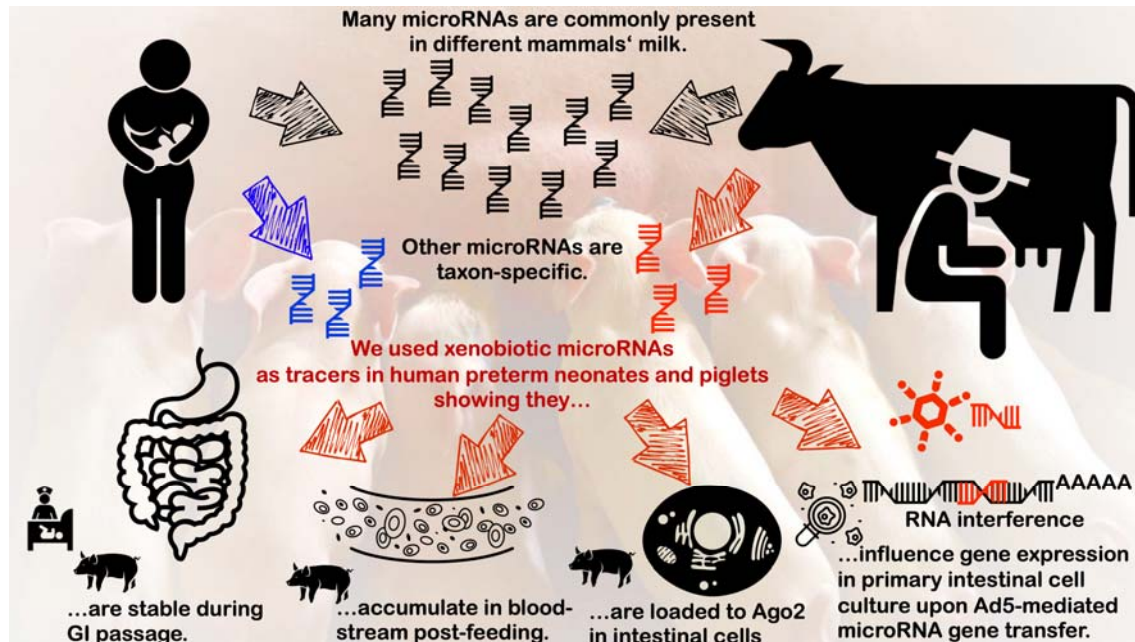
75 **Conclusions:** Taken together, our data point to a transmissibility of milk miRNA signals, which could
76 be relevant at least for intestinal maturation. Ad5-based miRNA-gene transfer into HIEC-6 revealed
77 putative milk miRNA targets on the protein and transcriptome levels. Results suggest that milk
78 miRNAs could influence gene expression in intestinal epithelia of neonates under special conditions.

79

80 **Key words**

81 intestinal maturation; enteral feeding; necrotizing enterocolitis; preterm delivery; fetal human
82 intestinal epithelial cells; preterm piglet; miRNA target

83 Graphical abstract



84

85 It is already known that exclusive breastfeeding is the best source of nutrition for neonates. Human breast
86 milk has a high miRNA content in comparison to other body fluids. It is controversially discussed whether
87 they could influence gene regulation in term and preterm neonates and thus might vertically transmit
88 developmental relevant signals. Here, we contribute important new findings: Mammals have in common a
89 significant number of milk miRNAs yet exhibit taxon-specific fingerprints. These differences allowed us to
90 exploit xenobiotic miRNAs as tracers in human preterm neonates, who routinely received formula-
91 supplemented nutrition in addition to breast milk. Tracer miRNAs survived the gastrointestinal (GI) transit
92 in human preterm neonates. In a preterm piglet model the reporter miRNA did not only survive GI transit,
93 but accumulated in the bloodstream few hours post-feeding. Moreover, we show that, cel-mir-39-5p and
94 cel-miR-39-3p became loaded to Ago2 in intestinal tissue samples, which is prerequisite for milk
95 microRNAs' biological relevance. Adenovirus type 5-based miRNA-gene transfer into HIEC-6 allowed us
96 to examine predicted bovine milk miRNA targets on the protein and transcriptome levels.

97 © Creative Commons Icons were downloaded from the Noun Project (<https://thenounproject.com/> [‘breastfeeding’ by Gan Khoon Lay from
98 the Noun Project; ‘milking’ by Laymik from the Noun Project; ‘digestive system’ by Design Science, US, in the Organs Collection;
99 ‘bloodstream’ by Oleksandr Panasovskyi, UA; ‘cell’ by Léa Lortal from the Noun Project; ‘RNA’ by Georgiana Ionescu from the Noun
100 Project; ‘pig’ by parkjisun from the Noun Project; ‘nursery’ by Luis Prado from the Noun Project; ‘arrow up’ by Alex Muravev from the
101 Noun Project; ‘cancer cells’ by dDara from the Noun Project; ‘adenovirus’ by Fariha Begum from the Noun Project]) and arranged for this
102 graphical abstract.

103

104 **Introduction**

105 Exploiting xenobiotic milk has a long history in human nutrition since the Neolithic revolution and left
106 marks in contemporary human genomes. Whereas most native European hunter gatherers apparently
107 exhibited lactase (LCT) non-persistence post-weaning, dairy farming practiced by immigrating
108 Neolithic cultures came along with genetic adaptations associated with LCT persistence post-infancy.
109 Apparently, domestication of mammals led to a beneficial niche construction, where those adaptations
110 allowed to exploit xenobiotic milk as additional food source [1-5]. Particularly bovine milk has a
111 global role for human nutrition to date and in addition to fresh milk, industrialized dairy products play
112 an important role in the global market [6], e.g. in the form of powdered milk or formula nutrition for
113 neonates. In preterm neonates it is observed that LCT activity increases after the begin of enteral
114 feeding with formula-fed infants exhibiting lower lactase activity levels than milk-fed infants [7]. One
115 possible explanation is that milk vs. formula feeding can differently influence the epigenetic LCT
116 regulation. In a preterm piglet model supplementation with formula or bovine colostrum led to
117 differential intestinal gene expression patterns, when compared to total parenteral nutrition [8].
118 Importantly, enteral feeding influences the risk for necrotising enterocolitis (NEC) in preterm infants.
119 NEC susceptibility increases in premature infants and piglets receiving xenobiotic formula milk when
120 compared to breast milk/colostrum feeding [9-12]. However, the molecular background of nutrition-
121 dependent differences in gene regulation remains concealed.
122 Whereas the chromatin structure controls transcriptional gene silencing (TGS), post-transcriptional
123 gene silencing (PTGS) utilizes RNA interference (RNAi), sometimes at important nexus in
124 hierarchical gene regulatory networks (Figure S1). RNAi key factors are non-coding microRNAs
125 (miRNAs) interacting with Argonaute (Ago) protein family members to target specific mRNAs via
126 base-pairing of their 5'-seed [13-15]. Perfect or near-perfect base-pairing promotes the decay of
127 targeted mRNAs, whereby translational repression seems to be another mechanism of PTGS [16]. In
128 cells, miRNAs fulfil important regulatory functions, but they occur also ubiquitously in body fluids.
129 Among different body fluids, human breast milk seems to exhibit the highest total miRNA
130 concentration [17]. Also, miRNAs are found in processed milk- products, such as formula milk [18].
131 There is an ongoing debate in science and society about possible adverse effects of milk consumption

132 with particular emphasis on bovine milk and in some instances focussing the controversy on its
133 miRNAs content [19-21]. But the discussion suffers from a lack of comparative and experimental data
134 about the biological relevance of milk miRNAs. One exception was an elegant approach looking at the
135 intestinal uptake of milk miRNAs in mmu-mir-375-knockout and mmu-mir-200c/141-knockout mice
136 offspring, which received milk from wild-type foster mothers. Here, no evidence for intestinal
137 epithelial uptake of miRNA and/or its enrichment in blood, liver and spleen was seen [22].
138 Contradicting results were obtained from another study that simulated infant gut digestion *in vitro* and
139 analysed the uptake of human milk miRNAs by human intestinal epithelial crypt-like cells (HIEC)
140 deriving from foetal intestines at mid-gestation. Here, milk miRNA profiles remained stable after
141 digestion and evidence for the uptake of milk-derived exosomes in HIEC was reported [23]. There is
142 an urgent need for further rigorous experimental data to inspire the debate and address the open
143 problems: Are milk miRNAs functional, or are they a nucleo(t/s)ide source, only? We currently
144 neither know whether milk miRNAs build a path of vertical signal transmission from mother to the
145 new-born nor whether interferences of xenobiotic miRNAs with human target mRNAs can influence
146 developmental pathways [24]. We thus aimed to interrogate the potential relevance of human and
147 xenobiotic milk miRNAs in specific situations in early human life.

148

149

150 **Results and Discussion**

151 We followed the working hypothesis that breast milk miRNAs could fulfil a regulatory signalling
152 function, which could be most important within a discrete perinatal ‘window of opportunity’ during
153 the introduction of enteral feeding, when the infant’s intestine develops as an environment-organism
154 interface to coordinate microbiome homeostasis. Moreover, we considered that intestinal immaturity
155 in preterm neonates could provide a clinically significant niche for (xenobiotic) milk miRNA
156 influence.

157

158 *Mammals have in common a large number of milk miRNAs yet exhibit species-specific milk miRNA*
159 *fingerprints*

160 We determined milk miRNA profiles of human (hsa), cattle (bta), goat (cae), and sheep (ogm) to
161 clarify a potential role of miRNA molecules in dietary milk. Furthermore, milk miRNAs from pig
162 (ssc), okapi (oyo), horse (eca), donkey (eas), cat (fca), and dog (clu) were considered to possibly derive
163 an evolutionary context of their profiles, for example putative milk miRNA differences between
164 omnivores, herbivores, and carnivores (Figure 1A). The top 100 milk miRNAs from 21 specimens
165 representing <90% of the total mapped miRNA read counts (92.40-96.39%) were visualized as heat
166 map and dot plot (Figure 1B,C). Across all taxa we detected 1291 hairpin-like pre-miRNAs (pre-mir),
167 whereby each single pre-mir could potentially give rise to two mature single-stranded mature miRNAs
168 (miR) through processing of its guide (5p) and/or passenger (3p) strand. 139 of these pre-mirs
169 occurred in all taxa.

170 Robustly, the heat map suggested a stable quantitative distribution of most miRNAs in most species'
171 milk, whereby principal component analyses revealed somewhat separated clusters: Cluster 'blue'
172 contained all human specimens, cluster 'green' contained all herbivores as well as dog, whereas pig
173 and cat appeared somewhat separated (Figure S2). Using ANOVA for deeper investigation of the
174 putative differences between hsa-miRs and bovid miRs, we identified only few differences with solely
175 miR-192-5p being $p < 0.0001$ and 3 miRs being below $p < 0.05$ (miR-1246, miR-146b-5p, miR-4516).
176 Similarly, few differences were seen, when we compared hsa-miRs vs. ssc-miRs, bovid miRs vs. ssc-
177 miRs, omnivores miRs vs. herbivores miRs, omnivores miRs vs. carnivores miRs and herbivores miRs
178 vs. carnivores miRs (Table S1).

179 Apart, numerous miRNAs were apparently shared by some taxa or occurred taxon-specific. Through
180 their annotations and Blast searches in miRBase [25], we undertook an approach to systematically
181 identify taxon-specific pre-mir and to analyse their non-overlapping or partially overlapping
182 occurrence in different taxa (Table S2). For each taxon, we identified several hundreds of milk pre-
183 mirs (carnivores: $n=240$; bovinds: $n=521$; human: $n=679$; pigs: $n=272$; equids: $n=381$) (Figure 1D).
184 Notably, 225 pre-mir were shared between humans and cattle. We found 440 pre-mir being human-
185 specific, 270 being bovinds-specific and many more taxon-specific pre-mir (pigs [$n=91$], equids
186 [$n=172$] and carnivores [$n=240$]). We concluded that xenobiotic miRNAs could be exploited as tracers

187 to study the gastrointestinal (GI) passage as well as systemic and cellular uptake in human or animal
188 models.

189

190 *Cattle-specific milk miRNA can potentially target human mRNA*

191 To study the GI passage of milk miRNAs we selected dietary *Bos taurus* (bta)-specific (pre-) miRNAs
192 as tracers. The 50 top-ranked bovid-specific pre-mir were used for heat map illustration (specimens: 8
193 cattle, 1 yak, 1 water buffalo) (Figure 1E; left column). Further, 11 formula/powdered milk products
194 are shown (compare Table S3A) (Figure 1E; right column). Most bovid-specific pre-mir from liquid
195 milk were present in formula products with similar relative quantities, but mostly with lower total
196 miRNA concentrations in formula (Figure 1F).

197 For deeper investigation of their putative influence in a human host we selected several bta-miRs
198 using relative quantities and the validated the absence of similar miRs in the human miRNome as the
199 main selection criteria (Figure 1E, red font). Selected bta-miRNA quantities were estimated via their
200 ranks (#n) within *Bos taurus* total miRNAs: bta-mir-2904 (#19); bta-mir-2887 (#67); bta-mir-2478
201 (#93); bta-mir-3533 (#141); bta-mir-2428 (#169); bta-mir-2440 (#172); bta-mir-677 (#191); bta-mir-
202 2892 (#229); bta-mir-2404 (#232); bta-mir-2361 (#237); bta-mir-2372 (#278); bta-mir-2304 (#284).
203 Typically, human mRNA target prediction for those bta-miRNAs via miRDB [26] revealed dozens of
204 potential high scoring 3'-UTR targets, with transcripts of several master regulatory genes among them
205 (Table S4). For example, for bta-miR-677-5p (5'-CUCACUGAUGAGCAGCUUCUGAC-3',
206 probable seed-sequence underlined), transcription factor SP4, *zink finger and homeobox family*
207 *member 1* (ZHX1) and the chromatin remodeller ATRX were among the predicted human mRNA
208 targets (n=655). Importantly, such algorithms usually deliver large numbers of false-positive results,
209 which might be invalid for specific cell types-of-interest. But before interrogating this problem, it is
210 crucial to address whether (xenobiotic) miRNAs stay intact during the gastric and intestinal transit and
211 eventually do reach potential mRNA targets within cells.

212

213 *Dietary-derived bta-miRs survive gastrointestinal transit in human newborns*

214 Consistently, we examined a randomly selected preterm neonate stool sample collection from an
215 intensive care neonatology unit. The donors were given routinely formula supplementation (mean
216 gestational age: 29.2 wks [24.4-35.7]) [27]. Quantitative real-time PCR (qPCR) analyses were
217 performed using cDNA libraries prepared from purified small RNAs and specific sets of bta-miR or
218 pan-miR primer pairs (Table S3B). As a matter of fact, we detected intact all interrogated bta-miRs in
219 all pre-term stool samples (Figure 2A). This demonstrates that nutritional uptake of milk miRNAs
220 leads to their intestinal enrichment and suggests their stable sequence integrity during gastrointestinal
221 (GI) transit in human preterm neonates.

222

223 *Xenobiotic miRNAs become enriched in preterm piglets' intestinal cells following 9-days enteral*
224 *nutrition with bovine colostrum or formula*

225 We studied intestinal cellular uptake of milk miRNAs in vivo exploiting bovine colostrum or formula
226 derived bta-miRs as tracers in a preterm neonate piglet model wherein the effects of enteral feeding
227 introduction post-delivery are subject of comprehensive ongoing studies [8-12]. Following 9 days of
228 bovine colostrum or formula supplementation after the introducing enteral feeding a protocol for
229 intestinal epithelial cell enrichment was applied prior to miRNA library preparation and deep
230 sequencing. Strikingly, we found 4 bta-miRs, which became enriched within the 50 top-ranked
231 intestinal cellular miRNAs (Figure 3A). Thereby, bta-miR-2904 occupied rank #4 suggesting that a
232 dietary miRNA could in principle reach biologically significant levels if being taken up by cells.
233 Apparently, the rate of cellular uptake was partly influenced by the bta-miR abundance in bovine milk
234 (bta-miR-2904: #4 in intestinal cells (IC) vs. #1 (bta-specific miRs) in bovine milk (BM); bta-miR-
235 2881: #31/not ranked in IC/BM; bta-miR-2892: #37/6 in IC/BM; bta-miR-2887: #39/2 in IC/BM;
236 compare Figure 1E). It might be notable that none of the interrogated bta-miRs was detected in
237 cerebrospinal fluid samples from piglets receiving enteral feeding of bovine colostrum [28],
238 suggesting their limited blood-to-cerebrospinal fluid permeability or, respectively, indicating that they
239 did not reach detectable concentrations. Apart, we note that for the many miRNAs with identical
240 sequences in different taxa an endogenous or food-derived origin might be impossible to discriminate.

241

242 *In neonatal preterm piglets feeding with cel-miR-39-5p/-3p-supplemented colostrum bolus leads to*
243 *bloodstream enrichment of reporter miRNAs*

244 Following the observation that 9-days-feeding leads to xenobiotic miR enrichment in intestinal cells of
245 neonate piglets, we interrogated whether milk miRNAs could possibly also be involved as regulators
246 in the development of gut homeostasis or other developmental processes, which start perinatally or
247 early postnatally. Therefore, we studied whether and how fast dietary colostrum bolus
248 supplementation with reporter miRNAs (cel-miR-39-5p and cel-miR-39-3p [Figure 3B]) can lead to
249 bloodstream accumulation of xenobiotic cel-miR tracers after GI transit utilizing the preterm piglet
250 model. At different time points post-feeding ($t_1=30$ min, $t_2=1$ h, $t_3=2$ h, $t_4=3$ h, $t_5=5$ h and $t_6=7$ h)
251 peripheral blood was sampled. Then total serum RNA was used for miRNA library preparation and
252 successive analyses of enrichment of both reporter cel-miRNAs by qPCR. MicroRNA-seq was
253 conducted from serum sampled 7 h post-feeding for confirmation. Along most time points of
254 sampling, we did not observe qPCR signals above threshold, but 7 h post feeding the signal for cel-
255 miR-39-3p massively increased (Figure 3B) suggesting the transit of considerable amounts of cel-
256 miR-39-3p from the GI tract into the bloodstream. At this timepoint enrichment was not observed for
257 cel-miR-39-5p. Reads for cel-miR-39-3p could be verified by miRNA-seq, which was reminiscent of
258 the cel-miR-39-3p/5p-bias observed in qPCR analyses before (Figure 3C), but reasons remain unclear.
259 Remarkably, the timing of reporter miRNA accumulation in serum very roughly appeared to be in
260 agreement with GI transit times of radiotracers in suckling piglets (21 days old; approx. 1.5-3.5 h until
261 75% of gastric emptying and >9.5 h until 75% intestinal emptying) [29].

262

263 *Dietary supplemented cel-miR-39-5p and cel-miR-39-3p co-precipitate with Ago2*

264 The biological activity of miRNAs requires their loading into Ago2-containing protein complexes. We
265 analysed whether cel-miR-39-5p/-3p miRNAs can be pulled-down from piglet intestinal biopsies 7h
266 post-feeding using the anti-pan-Ago2 monoclonal antibody (Sigma-Aldrich, MABE56, clone 2A8).
267 Both cel-miR-39-5p as well as cel-miR-39-3p could be detected in Ago2-precipitates from pre-term
268 piglets, which were fed with reporter-miRNA-supplemented colostrum, suggesting that Ago2 in
269 intestinal cells can be loaded with both the guide and the passenger strands resulting from processed

270 cel-mir-39 (Figure 3D). Remarkably, the stronger signal for cel-miR-39-3p was reminiscent of its
271 predominant enrichment in the bloodstream 7h post-feeding. Due to the presence of positive cel-miR-
272 39-5p qPCR signals in Ago2-immunocomplexes we assume that its bloodstream enrichment could
273 simply lag behind cel-miR-39-3p instead of being selectively excluded.

274

275 *Weak evidence for DDX3 targeting through bta-mir-677 in HIEC-6 cells is superimposed by several*
276 *probable false-positive predictions of miRNA-mRNA interactions*

277 If anticipating a vertical transmission of PTGS via milk miRNAs, the superordinate problem is which
278 mRNAs are true targets. Clearly, target prediction depending mostly of 5'-seed complementarity
279 remains leaky for simple reasons: First, because searches for sequence matches in mRNA databases
280 usually cannot consider whether a potential target is transcribed in a cell or tissue-of-interest or not.
281 Second, prediction algorithms do not consider that within a cell different miRNAs and mRNAs
282 compete for being loaded to a limited number of Argonaute (Ago) proteins [30]. Moreover, given that
283 mRNA decay and blocking of translation exist as alternative miRNA interference mechanisms, it is
284 not clear whether PTGS can be detectable directly on the mRNA level and/or the protein level only.
285 Consequently, the identification of valid miRNA-target interactions and their influence on gene
286 regulatory networks requires detailed experimental analyses.

287 We thus studied the potential influence of bta-mir-677 on bioinformatically predicted human targets in
288 primary foetal human intestinal epithelial cells (HIEC-6) using adenovirus type 5 (Ad5)-based miRNA
289 gene transfer. Using this transduction method, we efficiently overcame the disadvantageous signal-to-
290 noise ratio of standard transfection protocols (Figure S3). Transcriptome profiling confirmed that this
291 model well fulfilled important criteria for the purpose of miRNA experiments in non-transformed
292 cells, which retained foetal epithelial cell characteristics under primary cell culture conditions and
293 under the influence of Ad5-mediated miRNA transfer (Figure 4A). From the list of predicted human
294 mRNA targets of bta-miR-677-5p, we selected ATRX, DDX3, PLCXD3 and ZHX1 for analyses by
295 immunofluorescence microscopy and quantitative Western blots (Figure 4B,C). These targets had a
296 high miRDB scores, and they were annotated being potential master regulatory genes. However, from
297 this unavoidably arbitrarily selection, none of the candidates exhibited differences in the quantity or

298 subcellular distribution using microscopy (Figure 4B). On the scale of whole cell populations, we
299 conducted quantitative Western blot analyses. Interestingly, for DDX3, analyses of two Western blots
300 revealed a 24.45% reduction (SD: $\pm 1.68\%$) of DDX3 signals in bta-mir-677-treated vs. wild-type and
301 a 37.90% (SD: $\pm 1.90\%$) DDX3 signal reduction in bta-mir-treated vs. ctrl-mir-treated HIEC-6. These
302 results suggested that bta-mir-677 expression in HIEC-6 cells could indeed influence the expression of
303 one of the predicted human mRNA targets, leading to reduced translated DDX3 protein. Even though
304 the latter observation could give some hint for an influence of bta-miR-677-5p in HIEC-6 cells, the
305 relative arbitrary putative target selection and laborious validation is unrewarding and non-holistic.
306 We therefore analysed the influence of Ad5-mediated miRNA gene transfer using four different
307 bovine miRNAs-of-interest (miRoI) (bta-miR-677-5p, bta-miR-2404-5p, bta-miR-2440-3p and bta-
308 miR-2361). We determined the fold-changes of all transcribed genes in miRoI-treated cells with
309 reference to non-sense miR-treated HIEC-6. For comparison, we then focussed our analyses on all
310 expressed predicted target genes of each miRoI with reference to non-sense miR-treated HIEC-6
311 (Figure 4D). Whereas most genes remained unaffected by miRoI-treatment, we observed numerous
312 significant cases of downregulation within the group of predicted miRoI targets (Median fold-changes
313 all transcripts/predicted targets: bta-miR-677-5p: 0.9908/0.8147 [$p < 0.0001$]; bta-miR-2404-5p:
314 0.9805/0.9587 [$p = 0.0032$]; bta-miR-2440-3p: 1.0070/0.9728 [$p = 0.0240$]; bta-miR-2361-5p:
315 1.0340/0.9361 [$p < 0.0001$]), whereby we did not see any correlation between the degree of observed
316 downregulation and the individual position/score as a result of target predictions.

317

318 Taken together, our experimental trajectory suggests that dietary uptake of milk miRNAs can lead to
319 their loading to Ago2 in neonatal intestinal epithelial cells. Thus, vertical transmission of maternal
320 milk miRNA signals via GI transit to responsive cells and systemic bloodstream distribution is
321 apparently possible. This is in agreement with the ‘functional hypothesis’, but contradicts the ‘non-
322 functional’ hypothesis that milk miRNAs could solely serve as a nucleoside source for the newborn
323 [31]. Our results from tracer experiments provide good experimental justification to address
324 superordinate questions about milk miRNA-induced PTGS in neonates. However, key problems
325 remain and should be addressed: We have no idea, which of the hundreds of different miRNAs found

326 in milk with different abundance could be important and how selective loading of Ago2 in milk
327 miRNA-responsive cells could work. Possibly, only some specific miRNAs find specific mRNA
328 duplex partners, depending on their presence in specific cell types and transcriptional timing.
329 Systemically, it remains unknown how far-reaching milk miRNAs' influence could be. Could
330 biologically relevant miRNA accumulation be restricted to the intestine, or does their observation in
331 the bloodstream indicate a systemic distribution to other target tissues/cells? As important as the place
332 of milk miRNA activity is the time of action during ontogeny. Most convincing could be the existence
333 of a relatively narrow 'window of opportunity', which could open perinatally and could persist during
334 the introduction of enteral feeding, when the infant's intestine develops as an environment-organism
335 interface to coordinate microbiome homeostasis.
336 In HIEC-6, we have efficiently applied Ad5-mediated gene transfer, establishing continuous, but
337 probably non-natural cellular levels of ectopically expressed miRNAs. This might lead to enforced
338 Ago2-loading caused by outnumbered availability of the substrate (dog-eat-dog effect). These
339 conditions may not fully reflect the in vivo situation in the neonate intestine, but nevertheless might be
340 useful to study the influence of (xenobiotic) milk miRNAs on gene regulatory networks. This
341 approach could plausibly help to explain the observed increase of severe intestinal complications such
342 as NEC in premature infants fed with bovine based formula milk. However, we clearly emphasize that
343 postulating potential harmful influence would be an overstated conclusion from our experiments. But
344 for the first time in human history, the newest developments in intensive care neonatology allow the
345 survival of extremely vulnerable preterm neonates, whereby severe complication are often associated
346 with incomplete intestinal development. Thus, if the 'window of opportunity' hypothesis discussed
347 above holds, the consideration of xenobiotic milk miRNA side effects on early preterm and term
348 neonatal development seems well justified and would encourage advanced future studies.

349
350

351 **Materials and Methods**

352 [Clinical trial registration](#)

353 All analyses including those using human faecal specimens were considered exploratory. Clinical trial
354 registration was not required since participants were not prospectively assigned to an intervention, the
355 research was not designed to evaluate the effect of an intervention on the participants, and no effect
356 was being evaluated in an health-related biomedical or behavioural outcome.

357

358 Samples and animal procedures

359 Human milk and stool specimens were collected with approval of the Witten/Herdecke University
360 Ethics board (No. 41/2018) after informed written consent was obtained by all involved donors.
361 Animal milk was purchased or collected with the help of Wuppertal Zoo, local farmers, or veterinary
362 medics. All animal procedures were approved by the National Council on Animal Experimentation in
363 Denmark (protocol number 2012-15-293400193). Piglet (landrace × large white × duroc; delivered by
364 caesarean section on day 105 [90%] of gestation) blood and gut biopsies derived from an experimental
365 ongoing series described previously [8]. For reporter miRNA supplementation of bovine colostrum
366 bolus for piglet feeding reported milk nucleic acids concentration were used as guideline (23 mg/L ±
367 19 mg/L [8.6-71 mg/L]) [32]. We supplemented bovine colostrum bolus with RNA oligonucleotides
368 mimicking both putatively processed strands of *Caenorhabditis elegans* (cel), cel-miR-39-5p and cel-
369 miR-39-3p, and adjusted their amount to achieve approx. 5-10% of human milk's total nucleic acids
370 content. Three neonatal low-birth-weight piglets from the same litter (mean birth weight 1,119 g
371 [1,071-1,167 g]; normal birth weight approx. 1,400-1,500 g) received initial feeding (t_0) of bovine
372 colostrum bolus (15 mL/kg) enriched with 39 g/L casein glycomacropeptide (CGMP), 2.8 g/L
373 osteopontin (OPN) and a mix of cel-miR-39-5p/-3p reporter miRNAs. As control, three other piglets
374 from the same litter received colostrum bolus without reporter miRNA supplementation (mean birth
375 weight 1,047 g [862-1,240 g]). After 2.5 h, the piglets received another bolus to facilitate gut motility.
376 At different time points post-feeding ($t_1=30$ min, $t_2=1$ h, $t_3=2$ h, $t_4=3$ h, $t_5=5$ h and $t_6=7$ h) 1 mL
377 peripheral blood was sampled. Total RNA was used for miRNA library preparation and successive
378 analyses of enrichment of both reporter cel-miRNAs by qPCR, whereas confirmatory miRNA-seq was
379 conducted 7 h post-feeding only.

380 Enrichment of piglet intestinal epithelial cells from intestinal mucosa biopsies was done as follows.
381 Pigs were euthanised using 200 mg/kg intraarterial sodium pentobarbital after anaesthesia
382 administration. The GI tract was immediately removed, and the small intestine was carefully emptied
383 of its contents. 30 cm of the distal small intestine were used for cell collection. The segment was
384 flushed with 10 mL of pre-chilled NaCl 0.9% (Fresenius Kabi, Uppsala, Sweden) and then cut open
385 along the length. The upper layer of the intestinal mucosa was gently scraped off with a microscopic
386 slide and transferred in a 15 mL tube containing 12.5 mL PBS containing FBS (final concentration
387 1.12 μ L/mL). Homogenization was achieved by pipetting with a plastic Pasteur pipette for about 1 min
388 and then stirring the solution at 500 rpm for 20 min at room temperature. The homogenized
389 suspension was filtered through a 70 μ m cell sieve and spun down at 500 xg at 4°C for 3 min. The cell
390 pellet was resuspended in 5 mL modified PBS (see above), filtered and centrifuged again. The pellet
391 was then resuspended in 1 mL red blood cell lysis buffer (1x, Invitrogen™, ThermoFisher
392 Scientific), incubated for 5 min at room temperature and then spun down at 500 xg at 4°C for 3 min.
393 The cell pellet was washed again and finally resuspended in 1 mL modified PBS (see above). From
394 the resulting single cell suspension 250 μ L were used for RNA purification. The authors state that they
395 have obtained appropriate institutional review board approval or have followed the principles outlined
396 in the Declaration of Helsinki for all human or animal experimental investigations.

397

398 Nucleic acids

399 Total RNA was purified from milk serum, blood serum, radically grinded tissue, cells and stool
400 samples using Trizol reagent (Sigma, MO, USA) upon manufacturer's recommendations. RNA quality
401 and quantity were assessed by microcapillary electrophoresis using an Agilent Bioanalyzer 2100
402 similarly as described [33]. A list of oligonucleotides used is provided as appendix (Table S3A).

403

404 Real time PCR

405 Quantitative measurement of miRNAs was analysed from cDNA libraries (as described in [33]) using
406 primer pairs as listed (Table S3A) and the QuantiTect SYBR Green PCR Kit (Qiagen) using a Corbett
407 Rotor-Gene 6000 qPCR machine. Specifically, a combination of miR-specific forward primers

408 [bta/pan-miR-*name*-5p/-3p-fw] and library-specific reverse primers [library_P*n*_miR_rv]) was used
409 (Table S3B). PCR conditions were as follows: 95°C for 15 min, 40 cycles of (95°C for 15 s, 60°C for
410 30 s). Amplicon melting was performed using a temperature gradient from 55–95°C, rising in 0.5°C
411 increments. For relative comparative quantification of quantitative expression fold changes we utilized
412 the $\Delta\Delta C_t$ method [34] using stable miR-143-3p, miR-99b-5p and let7b-5p for normalization.

413

414 Deep sequencing of miRNAs (miRNA-seq) and bioinformatics pipeline

415 Small RNAs (18-36 nt) were purified from total RNA using polyacrylamide gel electrophoresis
416 (PAGE). The subsequent cDNA library preparation utilizes a four-step process starting with the
417 ligation of a DNA oligonucleotide to the 3'-end of the selected small RNAs, followed by ligation of a
418 RNA oligonucleotide to the 5'-end of the selected small RNAs. The resulting molecules were
419 transcribed via reverse transcription (RT) and amplified via PCR [33]. Subsequently, after final quality
420 checks by microcapillary electrophoresis and qPCR, the libraries were sequenced on an Illumina
421 HiSeq 2000 platform (single end, 50 bp). This work has benefited from the facilities and expertise of
422 the high throughput sequencing core facility of I2BC (Research Center of GIF –
423 <http://www.i2bc.paris-saclay.fr/>). The initial data analysis pipeline was as follows: CASAVA-1.8.2
424 was used for demultiplexing, Fastqc 0.10.1 for read quality assessment and Cutadapt-1.3 for adaptor
425 trimming, resulting in sequencing reads and the corresponding base-call qualities as FASTQ files. File
426 conversions, filtering and sorting as well as mapping, were done using 'Galaxy' [35-37], a platform
427 for data intensive biomedical research (<https://usegalaxy.org/>), or 'Chimira' [38], sRNAtoolbox [39]
428 or 'miRBase' [25], respectively. For selected bta-mir we used the miRDB custom option for sequence-
429 based prediction of potential human mRNA targets [26].

430

431 Argonaute co-immunoprecipitation (Co-IP)

432 Association of reporter cel-miR-39 co-fed with milk with Argonaute (Ago2) in piglet intestinal
433 biopsies was analysed using co-immunoprecipitation and qPCR. For native pan-Ago2 precipitation
434 from intestinal tissue we used monoclonal mouse anti-pan-Ago2 antibodies (Sigma-Aldrich,
435 MABE56, clone 2A8) similarly as described previously [40]. This antibody exhibits cross-species

436 reactivity with Ago2 from mouse, humans, and most probably from other mammals as well. After
437 final blood sampling 7-7.5 h post-feeding proximal and distal tissues were taken at euthanasia, deep
438 frozen at -20°C and shipped on dry ice. Prior to immunoprecipitation piglet intestinal tissue from a
439 liquid nitrogen storage tank was powdered using a Cellcrusher™ (Cellcrusher, Co. Cork, Ireland) pre-
440 chilled in liquid nitrogen. Subsequently, intestinal tissue powder was suspended in lysis buffer (20
441 mM Tris-HCl, pH7.5, 200 mM NaCl, 2.5 mM MgCl₂, 0.5% Triton X-100). Samples were incubated
442 overnight with 3 µg anti-pan-Ago (2A8) and 25 µL magnetic protein A beads (Diagenode). Following
443 the enrichment of immunocomplexes on a magnetic rack and several washes with PBS, the samples
444 were heated to 95°C for 15 min, and then RNA was purified from the immunocomplexes using Trizol
445 and isopropanol precipitation. Then RNA converted into cDNA libraries and cel-miR-39-5p/-3p were
446 analysed from cDNA libraries by qPCR.

447

448 Deep sequencing of miRNAs (miRNA-seq) and bioinformatics pipeline

449 Small RNAs (18-36 nt) were purified from total RNA using polyacrylamide gel electrophoresis
450 (PAGE). The subsequent cDNA library preparation utilizes a four-step process starting with the
451 ligation of a DNA oligonucleotide to the 3'-end of the selected small RNAs, followed by ligation of a
452 RNA oligonucleotide to the 5'-end of the selected small RNAs. The resulting molecules were
453 transcribed via reverse transcription (RT) and amplified via PCR [33]. Subsequently, after final quality
454 checks by microcapillary electrophoresis and qPCR, the libraries were sequenced on an Illumina
455 HiSeq 2000 platform (single end, 50 bp). This work has benefited from the facilities and expertise of
456 the high throughput sequencing core facility of I2BC (Research Center of GIF –
457 <http://www.i2bc.paris-saclay.fr/>). The initial data analysis pipeline was as follows: CASAVA-1.8.2
458 was used for demultiplexing, Fastqc 0.10.1 for read quality assessment and Cutadapt-1.3 for adaptor
459 trimming, resulting in sequencing reads and the corresponding base-call qualities as FASTQ files. File
460 conversions, filtering and sorting as well as mapping, were done using 'Galaxy' [35-37], a platform
461 for data intensive biomedical research (<https://usegalaxy.org/>), or 'Chimira' [38], sRNAtoolbox [39]
462 or 'miRBase' [25], respectively. For selected bta-mir we used the miRDB custom option for sequence-
463 based prediction of potential human mRNA targets [26].

464

465 Luciferase assay

466 We performed this experiment to rule out exemplarily that the observed bta-miR-candidates could be
467 simply miRNA-like sequence artefacts without any function, we interrogated whether bta-miR-677, a
468 candidate miRNA with intermediate abundance in milk can silence luciferase expression *in vitro* via a
469 predicted 3'-UTR target sequence in a human HeLa cell-based assay. Therefore, a SacI/NheI
470 fragment with sticky ends was hybridized from oligonucleotides through incubation in a boiling water
471 bath and successive chilling to room temperature (Table S3B). Then we cloned the fragment
472 containing a 7 bp 3'-UTR target motif reverse complementary to the 5'-seed (nucleotides 2-8) of bta-
473 miR-677-5p into the 3'-UTR region of the firefly luciferase gene (*luc2*) encoded in the pmirGLO dual
474 luciferase expression vector (Promega) (Figure S4A). For bioluminescence calibration this vector
475 contained a 2nd luciferase cassette (*Renilla*; hRluc-neo fusion). Subsequently, pmirGLO was co-
476 transfected into HeLa cells using Lipofectamin 2000 (ThermoFisher) with bta-mir-677-like hairpin
477 RNAs or non-luciferase directed controls, followed by bioluminescence quantification using a
478 GloMax® Multi Detection System (Promega). We observed very robust silencing of firefly luciferase
479 upon bta-mir-677-like co-transfection, suggesting that at least bta-miR-677-5p can function as valid
480 miRNA in human cells (Figure S4B).

481

482 Insertion of microRNA-hairpins into Ad5 vectors

483 To assess the effects of miRNA overexpression in cell culture Ad5-based replication deficient ΔE1
484 vectors harboring an hCMV promoter-driven expression cassette for the concomitant expression of
485 EGFP (as transduction marker) and miRNAs were generated based on the 'BLOCK-iT Pol II miR
486 RNAi Expression Vector Kits' protocol (Invitrogen). Vectors were serially amplified on 293 cells and
487 purified by CsCl density centrifugation. The vector titers were determined by OD260 and vector
488 genome integrity was confirmed by sequencing and restriction digest analysis [41]. Hairpins
489 mimicking bovine pre-mirs were designed to express miRNAs, which corresponded to bta-miR-677-
490 5p, bta-miR-2404-5p, bta-miR-2440-3p, bta-miR-2361-5p. Details of vector design can be obtained

491 upon request. The expression of bta-mir-677-like hairpins, bta-miR-677-5p and bta miR-677-3p,
492 respectively, was evaluated by qPCR using the Mir-X™ miRNA First Strand Synthesis Kit (Takara).

493

494 Cell culture and Ad5 transduction

495 Human intestinal epithelial cells (HIEC-6 [ATCC CRL-3266]) cells were cultured upon
496 manufacturer's recommendations. Flow cytometric analyses of HIEC-6 cells transduced with different
497 ranges of multiplicity of infection (MOI) were used to define a transduction efficiency and to
498 determine the optimal MOI (Figure S3). Considering transduction efficiency and compatibility, we
499 subsequently used MOI 10.000 in experimental routine. One day pre-transduction, 10⁶ HIEC-6 cells
500 were seeded in 6-well cell culture dishes. The following day, cells were washed with PBS, provided
501 with fresh medium and subsequently transduced with respective Ad5 vector particles. Cells were
502 harvested 96 h post-transduction. The expression of bta-mir-677-like hairpins, bta-miR-677-5p and
503 bta-miR-677-3p, respectively, was validated using the Mir-X™ miRNA First Strand Synthesis Kit
504 (Takara) in combination with qPCR. The results confirmed the expression of bta-mir-677-like
505 hairpins, bta-miR-677-5p, but a bias for bta-miR-677-3p suggesting preferential processing of the 5-p
506 guide strand (Figure S5). For Western blot analyses cell pellets were homogenized in RIPA buffer (50
507 mM Tris HCl pH 8.0, 150 mM NaCl, 1% NP-40, 0,5% sodium deoxycholate, 0,1% SDS plus
508 cOmplete™ Mini Protease Inhibitor Cocktail [Sigma-Aldrich]). Alternatively, cells were grown on
509 coverslips for immunofluorescence microscopy. Here, after Ad5-mediated miRNA transfer successful
510 expression of the miRNA transgene could be indirectly confirmed using immunofluorescence
511 microscopy and flow cytometry for detection of green fluorescent protein (GFP) that was co-expressed
512 with bta-mir-677-like hairpins from the same transcript.

513

514 Western blot analyses

515 Homogenized pellets were mixed with SDS. Proteins were separated by SDS-PAGE using 5%
516 stocking and 8% running gels and subsequently transferred to a nitrocellulose blotting membrane
517 (Amersham Protran Premium 0.45 μm NC). Membranes were blocked 1% BSA in TBST (20 mM
518 Tris;150 mM NaCl; 0.1% Tween 20; pH 7.4). Polyclonal rabbit anti-ATRAX (Abcam; ab97508),

519 polyclonal rabbit anti-DDX3 (Abcam; ab235940), polyclonal rabbit anti-ZHX1 (Abcam; ab19356),
520 polyclonal rabbit anti-PLCXD3 (Sigma-Aldrich; HPA046849), polyclonal rabbit anti-GAPDH
521 (Sigma-Aldrich; G8795) were used as primary antibodies at 1:500 dilution in blocking buffer, except
522 anti-GAPDH (dilution 1:20,000 in blocking buffer). For internal normalization anti-GAPDH was used
523 in parallel and simultaneously with each other primary antibody. Secondary antibodies were goat anti-
524 rabbit IRDye 800CW (LI-COR; 926-32211) and goat anti-mouse IRDye 680RD (LI-COR; 926-
525 68070), each being diluted 1:10,000 as a mix in blocking buffer. Fluorescence was monitored using
526 the Odyssey CLx Imaging system (LI-COR) with the 2-color detection option and analysed using
527 Image Studio software (LI-COR).

528

529 Immunofluorescence microscopy

530 5×10^5 HIEC-6 cells were grown on coverslips in 6-well plates and transduced as described above.
531 96 h post-transduction cells were fixed for 10 min in 2% PFA/DPBS, washed twice with DPBS and
532 then permeabilised using 0.5% Triton X-100/DPBS, followed by 0.1N HCl for exactly 5 min for
533 antigen retrieval and successive washes with DPBS. Blocking was done in 3% BSA/0.1% Triton
534 X100/DPBS. Subsequently, the primary antibodies were incubated in blocking buffer for 1 h/37°C: 1.
535 polyclonal rabbit anti-ATRAX (Abcam; ab97508) at 1:100, polyclonal rabbit anti-DDX3 (Abcam;
536 ab235940) at 1:500, polyclonal mouse anti-ZHX1 (Abcam; ab168522) at 1:100. Then polyclonal goat
537 anti-rabbit Cy3 (Jackson ImmunoResearch) or polyclonal goat anti-mouse Cy3 (Jackson
538 ImmunoResearch) were used as secondary antibodies, each at 1:100. Eventually, 4',6-diamidino-2-
539 phenylindole (DAPI) was used for DNA counterstaining at 0.1 $\mu\text{g}/\text{mL}$ followed by washes and
540 mounting with Prolong Gold (Invitrogen). Acquisition of images was done with a Nikon Eclipse Ti
541 Series microscope. Fluorochrome image series were acquired sequentially generating 8-bit grayscale
542 images. The 8-bit grayscale single channel images were overlaid to an RGB image assigning a false
543 color to each channel using open source software ImageJ (NIH Image, U.S. National Institutes of
544 Health, Bethesda, Maryland, USA, <https://imagej.nih.gov/ij/>).

545

546 Deep sequencing of messenger RNAs (mRNA-seq) and bioinformatics pipeline

547 Total RNA was purified from Ad5-transduced HIEC-6 cells expressing a nonsense-miR or bta-miRs
548 using Trizol reagent (Sigma, MO, USA) upon manufacturer's recommendations. RNA quality and
549 quantity were assessed by microcapillary electrophoresis using an Agilent Bioanalyzer 2100. All
550 specimens had a RIN between 8.9 and 9.2 and were subsequently used for sequencing library
551 preparation. Enrichment of mRNAs was done using the NEBNext Poly(A) mRNA Magnetic Isolation
552 Module (New England BioLabs, #E7490S) upon manufacturers' recommendations. Subsequently
553 cDNA libraries were prepared using the NEBNext Ultra II DNA Library Prep Kit for Illumina (New
554 England BioLabs, #E7645S) upon manufacturers' recommendations in combination with NEBNext
555 Multiplex Oligos for Illumina (Index Primer Set 1) (New England BioLabs, #E7335G). Before
556 multiplexing, library quality and quantity were assessed by microcapillary electrophoresis using an
557 Agilent Bioanalyzer 2100. Deep sequencing was done using an Illumina HiSeq2500. The initial data
558 analysis pipeline was as follows: CASAVA-1.8.2 was used for demultiplexing, Fastqc 0.10.1 for read
559 quality assessment and Cutadapt-1.3 for adaptor trimming, resulting in sequencing reads and the
560 corresponding base-call qualities as FASTQ files. File conversions, filtering and sorting as well as
561 mapping, were done using 'Galaxy' [35-37] (<https://usegalaxy.org/>), serially shepherding the FASTQ
562 files through the following pipeline of tools: 1. FASTQ groomer (Input: Sanger & Illumina 1.8+
563 FASTQ quality score type) [42]; 2. TopHat for gapped-read mapping of RNA-seq data using the short
564 read aligner Bowtie2 (Options: single end, Homo sapiens: hg38) resulting in a BAM formatted
565 accepted hits file [43]. 3. featureCounts to create tabular text file (Output format: Gene-ID "\t" read-
566 count [MultiQC/DESeq2/edgeR/limma-voom compatible]). 4. Prior to DESeq2 normalization, a
567 tabular file containing catalogued columns of read counts for all experiments was arranged in
568 Microsoft Excel for Mac 16.32. and then uploaded as a tabular text file to Galaxy. 5. annotadeMyIDs
569 was used to assign gene symbols and gene names to Entrez IDs. Biostatistical tests were carried out
570 using GraphPad Prism 8.4.3 software.

571

572

573 **Declarations and ethics statement**

574 Ethics approval

575 This study was conducted with approval of the Witten/Herdecke University Ethics board (No.
576 41/2018). All animal procedures were approved by the National Council on Animal Experimentation
577 in Denmark (protocol number 2012-15-293400193). The authors state that they have obtained
578 appropriate institutional review board approval or have followed the principles outlined in the
579 Declaration of Helsinki for all human or animal experimental investigations. In addition, for
580 investigations involving human subjects, informed consent has been obtained from all participants.
581 Patients or the public were not involved in the design, or conduct, or reporting, or dissemination plans
582 of our research
583

584 Informed consent statement

585 Informed written consent was obtained by all involved donors.
586

587 Data availability statement

588 The datasets generated and/or analysed during the current study are available in the NCBI BioProject
589 repository as fastq.gz files of miRNA-seq and mRNA-seq (SubmissionIDs: SUB7584111/
590 SUB9897357/BioProject ID: PRJNA740153/URL: <https://www.ncbi.nlm.nih.gov/bioproject/740153>).
591 The release date is 1.1.2022. Until then BioProject's metadata is available for reviewers at
592 <https://dataview.ncbi.nlm.nih.gov/object/PRJNA740153?reviewer=ak7p21hrpfc2c3j12617o58747>.
593

594 Competing interests statement

595 All authors declare that there is no conflict of interests.
596

597 Funding

598 This study was funded by the HELIOS Research Centre (JP) and the NEOMUNE research program
599 (PTS) from the Danish Research Councils. University of Copenhagen has filed a patent concerning the
600 use of bovine colostrum for groups of paediatric patients. The authors have no other relevant
601 affiliations or financial involvement with any organisation or entity with a financial interest in or
602 financial conflict with the subject matter or materials discussed in the manuscript apart from those
603 disclosed. No writing assistance was utilised in the production of this manuscript.
604

605 Authors' contributions

606 JP and PPW designed the study and wrote the paper. SR conducted Ad5-mediated miRNA gene
607 transfer experiments under supervision and with the help of FK, FJ and CH. Further, she prepared
608 mRNA-seq libraries. FK and JS developed the Ad5-mediated miRNA gene transfer. CAH traced
609 miRNAs in piglet blood and intestine and human stool. MA, AP and VO performed luciferase
610 experiments. Animal treatments as well as sample collection and preparation were done by DNN, PPJ
611 and PTS. PPW, FG, TT, MA, ACWJ and SW contributed to sampling of human and animal milk
612 specimens. PPW, FG, VW and CAH generated RNA libraries, conducted qPCR experiments and
613 NGS. JP and CAH performed Argonaute pull-down experiments. JP and PPW supervised
614 undergraduates and graduate students. JP supervised the study, analysed the data and wrote the
615 manuscript with the help of PPW, ACWJ, CH and FK.

616

617 Acknowledgements

618 We gratefully acknowledge Gilles Gasparoni (Institut für Genetik/Epigenetik, Universität des
619 Saarlandes, Germany) to enable and support our mRNA deep sequencing analyses under hard
620 conditions during the first European peak period of the SARS-CoV-2 pandemic. We further thank Dr.
621 Arne Lawrenz (director of Wuppertal Zoo) for providing Okapi (Lomela's) milk.

622

623

624 **References**

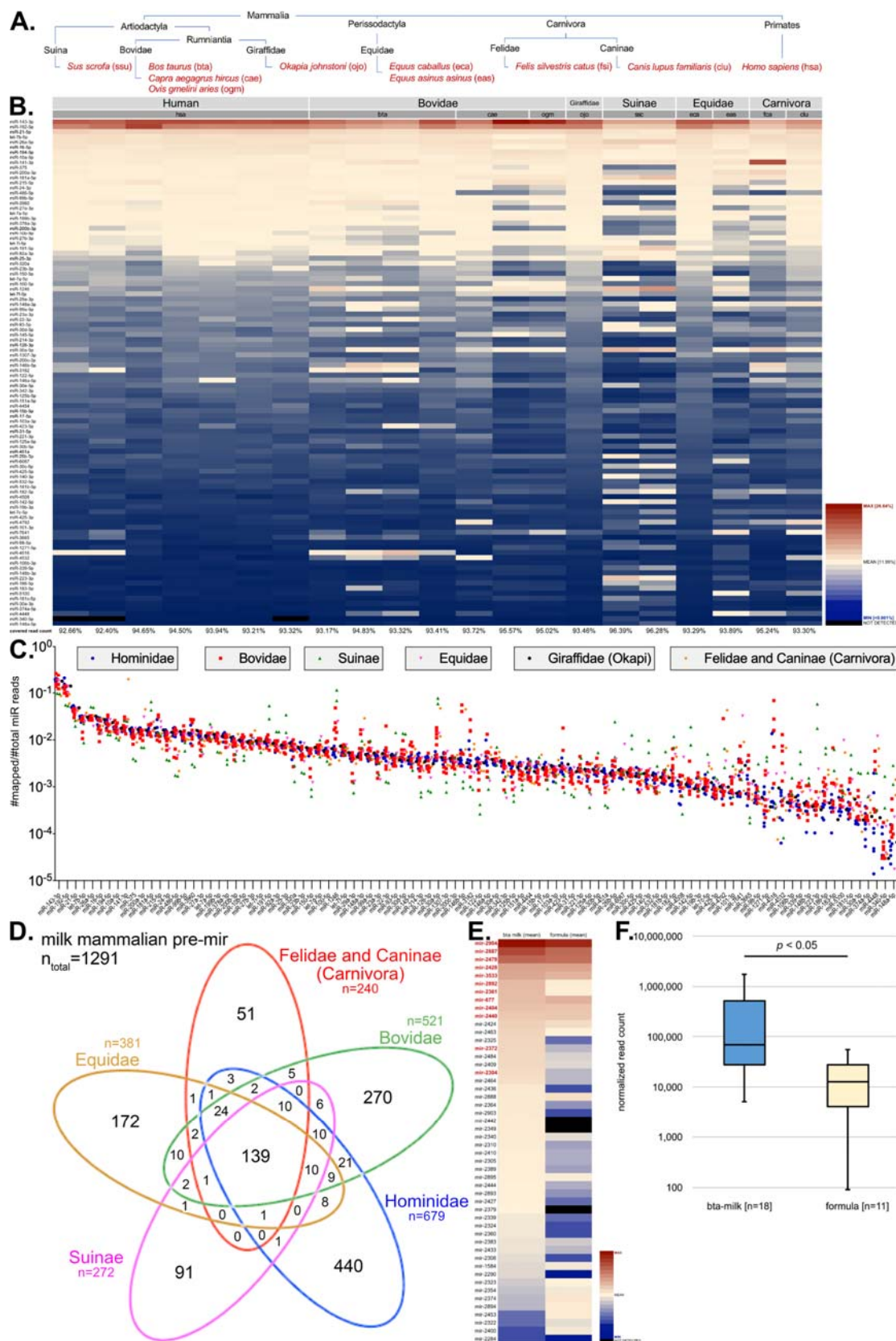
- 625 1. Brandt G, Szecsenyi-Nagy A, Roth C, et al. Human paleogenetics of Europe--the known
626 knowns and the known unknowns. *J Hum Evol.* 2015 Feb;79:73-92.
- 627 2. Gerbault P. The onset of lactase persistence in Europe. *Hum Hered.* 2013;76(3-4):154-61.
- 628 3. Segurel L, Bon C. On the Evolution of Lactase Persistence in Humans. *Annu Rev Genomics*
629 *Hum Genet.* 2017 Aug 31;18:297-319.
- 630 4. Beja-Pereira A, Luikart G, England PR, et al. Gene-culture coevolution between cattle milk
631 protein genes and human lactase genes. *Nat Genet.* 2003 Dec;35(4):311-3.
- 632 5. Gerbault P, Liebert A, Itan Y, et al. Evolution of lactase persistence: an example of human
633 niche construction. *Philos Trans R Soc Lond B Biol Sci.* 2011 Mar 27;366(1566):863-77.
- 634 6. Nuñez M. Existing Technologies in Non-cow Milk Processing and Traditional Non-cow Milk
635 Products. In: Tsakalidou E, Papadimitriou K, editors. *Non-Bovine Milk and Milk Products:*
636 *Academic Press;* 2016. p. 161-185.
- 637 7. Shulman RJ, Schanler RJ, Lau C, et al. Early feeding, feeding tolerance, and lactase activity in
638 preterm infants. *J Pediatr.* 1998 Nov;133(5):645-9.

- 639 8. Willems R, Krych L, Rybicki V, et al. Introducing enteral feeding induces intestinal
640 subclinical inflammation and respective chromatin changes in preterm pigs. *Epigenomics*.
641 2015;7(4):553-65.
- 642 9. Bjornvad CR, Schmidt M, Petersen YM, et al. Preterm birth makes the immature intestine
643 sensitive to feeding-induced intestinal atrophy. *Am J Physiol Regul Integr Comp Physiol*.
644 2005 Oct;289(4):R1212-22.
- 645 10. Lin PW, Stoll BJ. Necrotising enterocolitis. *Lancet*. 2006 Oct 7;368(9543):1271-83.
- 646 11. Moller HK, Thymann T, Fink LN, et al. Bovine colostrum is superior to enriched formulas in
647 stimulating intestinal function and necrotising enterocolitis resistance in preterm pigs. *Br J*
648 *Nutr*. 2011 Jan;105(1):44-53.
- 649 12. Sangild PT, Siggers RH, Schmidt M, et al. Diet- and colonization-dependent intestinal
650 dysfunction predisposes to necrotizing enterocolitis in preterm pigs. *Gastroenterology*. 2006
651 May;130(6):1776-92.
- 652 13. Bartel DP. MicroRNAs: target recognition and regulatory functions. *Cell*. 2009 Jan
653 23;136(2):215-33.
- 654 14. Brennecke J, Stark A, Russell RB, et al. Principles of microRNA-target recognition. *PLoS*
655 *Biol*. 2005 Mar;3(3):e85.
- 656 15. Chipman LB, Pasquinelli AE. miRNA Targeting: Growing beyond the Seed. *Trends Genet*.
657 2019 Mar;35(3):215-222.
- 658 16. Djuranovic S, Nahvi A, Green R. A parsimonious model for gene regulation by miRNAs.
659 *Science*. 2011 Feb 4;331(6017):550-3.
- 660 17. Weber JA, Baxter DH, Zhang S, et al. The microRNA spectrum in 12 body fluids. *Clin Chem*.
661 2010 Nov;56(11):1733-41.
- 662 18. Chen X, Gao C, Li H, et al. Identification and characterization of microRNAs in raw milk
663 during different periods of lactation, commercial fluid, and powdered milk products. *Cell Res*.
664 2010 Oct;20(10):1128-37.
- 665 19. Melnik BC. Milk: an epigenetic amplifier of FTO-mediated transcription? Implications for
666 Western diseases. *J Transl Med*. 2015 Dec 21;13:385.
- 667 20. Melnik BC. Milk disrupts p53 and DNMT1, the guardians of the genome: implications for
668 acne vulgaris and prostate cancer. *Nutr Metab (Lond)*. 2017;14:55.
- 669 21. Melnik BC, Schmitz G. Milk's Role as an Epigenetic Regulator in Health and Disease.
670 *Diseases*. 2017 Mar 15;5(1).
- 671 22. Title AC, Denzler R, Stoffel M. Uptake and Function Studies of Maternal Milk-derived
672 MicroRNAs. *J Biol Chem*. 2015 Sep 25;290(39):23680-91.
- 673 23. Kahn S, Liao Y, Du X, et al. Exosomal MicroRNAs in Milk from Mothers Delivering Preterm
674 Infants Survive in Vitro Digestion and Are Taken Up by Human Intestinal Cells. *Mol Nutr*
675 *Food Res*. 2018 Jun;62(11):e1701050.
- 676 24. Perge P, Nagy Z, Decmann A, et al. Potential relevance of microRNAs in inter-species
677 epigenetic communication, and implications for disease pathogenesis. *RNA Biol*. 2017 Apr
678 3;14(4):391-401.
- 679 25. Griffiths-Jones S, Grocock RJ, van Dongen S, et al. miRBase: microRNA sequences, targets
680 and gene nomenclature. *Nucleic Acids Res*. 2006 Jan 1;34(Database issue):D140-4.
- 681 26. Chen Y, Wang X. miRDB: an online database for prediction of functional microRNA targets.
682 *Nucleic Acids Res*. 2020 Jan 8;48(D1):D127-D131.
- 683 27. Zoppelli L, Guttel C, Bittrich HJ, et al. Fecal calprotectin concentrations in premature infants
684 have a lower limit and show postnatal and gestational age dependence. *Neonatology*.
685 2012;102(1):68-74.
- 686 28. Muk T, Stensballe A, Pankratova S, et al. Rapid Proteome Changes in Plasma and
687 Cerebrospinal Fluid Following Bacterial Infection in Preterm Newborn Pigs. *Front Immunol*.
688 2019;10:2651.
- 689 29. Snoeck V, Huyghebaert N, Cox E, et al. Gastrointestinal transit time of nondisintegrating
690 radio-opaque pellets in suckling and recently weaned piglets. *J Control Release*. 2004 Jan
691 8;94(1):143-53.
- 692 30. Janas MM, Wang B, Harris AS, et al. Alternative RISC assembly: binding and repression of
693 microRNA-mRNA duplexes by human Ago proteins. *RNA*. 2012 Nov;18(11):2041-55.

- 694 31. Melnik BC, Kakulas F, Geddes DT, et al. Milk miRNAs: simple nutrients or systemic
695 functional regulators? *Nutr Metab (Lond)*. 2016;13:42.
- 696 32. Thorell L, Sjoberg LB, Hernell O. Nucleotides in human milk: sources and metabolism by the
697 newborn infant. *Pediatr Res*. 1996 Dec;40(6):845-52.
- 698 33. Weil PP, Jaszczyszyn Y, Baroin-Tourancheau A, et al. Holistic and Affordable Analyses of
699 MicroRNA Expression Profiles Using Tagged cDNA Libraries and a Multiplex Sequencing
700 Strategy. *Methods Mol Biol*. 2017;1654:179-196.
- 701 34. Livak KJ, Schmittgen TD. Analysis of relative gene expression data using real-time
702 quantitative PCR and the 2(-Delta Delta C(T)) Method. *Methods*. 2001 Dec;25(4):402-8.
- 703 35. Blankenberg D, Von Kuster G, Coraor N, et al. Galaxy: a web-based genome analysis tool for
704 experimentalists. *Curr Protoc Mol Biol*. 2010 Jan;Chapter 19:Unit 19 10 1-21.
- 705 36. Giardine B, Riemer C, Hardison RC, et al. Galaxy: a platform for interactive large-scale
706 genome analysis. *Genome Res*. 2005 Oct;15(10):1451-5.
- 707 37. Goecks J, Nekrutenko A, Taylor J, et al. Galaxy: a comprehensive approach for supporting
708 accessible, reproducible, and transparent computational research in the life sciences. *Genome*
709 *Biol*. 2010;11(8):R86.
- 710 38. Vitsios DM, Enright AJ. Chimira: analysis of small RNA sequencing data and microRNA
711 modifications. *Bioinformatics*. 2015 Oct 15;31(20):3365-7.
- 712 39. Aparicio-Puerta E, Lebron R, Rueda A, et al. sRNAbench and sRNAtoolbox 2019: intuitive
713 fast small RNA profiling and differential expression. *Nucleic Acids Res*. 2019 Jul
714 2;47(W1):W530-W535.
- 715 40. Nelson PT, De Planell-Saguer M, Lamprinaki S, et al. A novel monoclonal antibody against
716 human Argonaute proteins reveals unexpected characteristics of miRNAs in human blood
717 cells. *RNA*. 2007 Oct;13(10):1787-92.
- 718 41. Kratzer RF, Kreppel F. Production, Purification, and Titration of First-Generation Adenovirus
719 Vectors. *Methods Mol Biol*. 2017;1654:377-388.
- 720 42. Blankenberg D, Gordon A, Von Kuster G, et al. Manipulation of FASTQ data with Galaxy.
721 *Bioinformatics*. 2010 Jul 15;26(14):1783-5.
- 722 43. Kim D, Pertea G, Trapnell C, et al. TopHat2: accurate alignment of transcriptomes in the
723 presence of insertions, deletions and gene fusions. *Genome Biol*. 2013 Apr 25;14(4):R36.
- 724

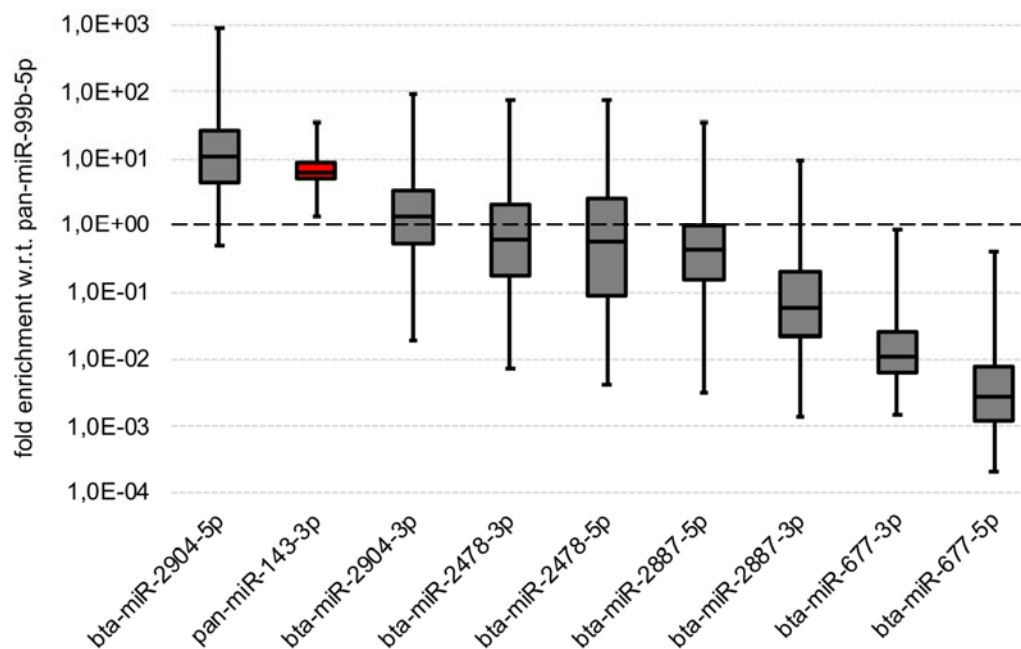
725

726 **Figures and captions**



727

728 **Figure 1. Comparative profiling of mammalian milk miRNAs. A.** Phylogenetic tree of specimens
729 under analysis (red font), which included mostly domesticated species with the exception of okapi
730 (ojo) and human (hsa). Additionally, we determined miRNA profiles from yak cheese and water
731 buffalo cheese (light red font), which are part of the available dataset, but are not part of the below
732 analyses due to insufficient total read counts and quality. **B.** Heat map of miRNAs conserved in all
733 taxa analysed. Only the top 100 miRNAs found in all species are shown robustly representing over
734 90% of the total read count in all specimens (see values below each column). A colour gradient was
735 used for the visualisation of each miRNA's abundance (read counts per million; CPM) in each
736 specimen. MicroRNAs were sorted in descending order with reference to the median CPM of human
737 specimens. **C.** The chart illustrates the quantitative distribution of the same top 100 miRNAs shown in
738 the above heat map. **D.** Venn diagram showing that the numbers of pre-miRNAs (pre-mir) shared by
739 all or some taxa or, respectively, which were identified being taxon-specific. For this analysis pre-mir
740 counts were used rather than miR-counts to counteract a potential differential taxon-specific 5p-/3p-
741 dominant processing. **E.** Heat map of the top 50 *Bos taurus* (bta)-specific pre-mir in raw and
742 industrially processed milk specimens (n=18) in comparison with powdered milk/formula product
743 specimens (n=11). The median CPM (mapped reads count per million) was used as sorting criterion in
744 descending order. Red font: miRNA was used for human mRNA target prediction via the sequence-
745 based custom prediction option of miRDB [26]. Cave! Bovidae in heat map include goat and sheep,
746 whereas ranks were determined from cattle only. **F.** Quantitative analysis of total miRNA read counts
747 in raw and industrially processed milk specimens (n=18) in comparison with powdered milk/formula
748 product specimens (n=11).
749
750
751
752

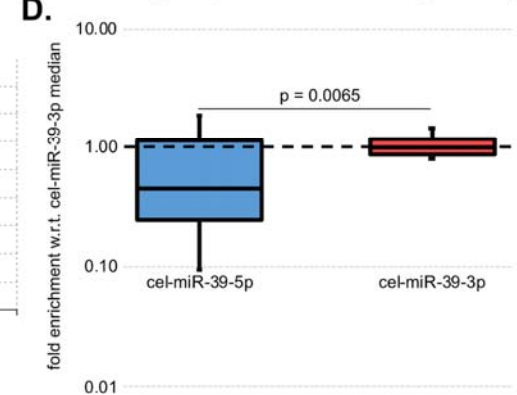
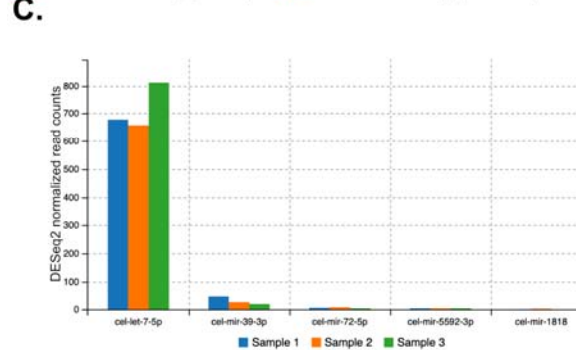
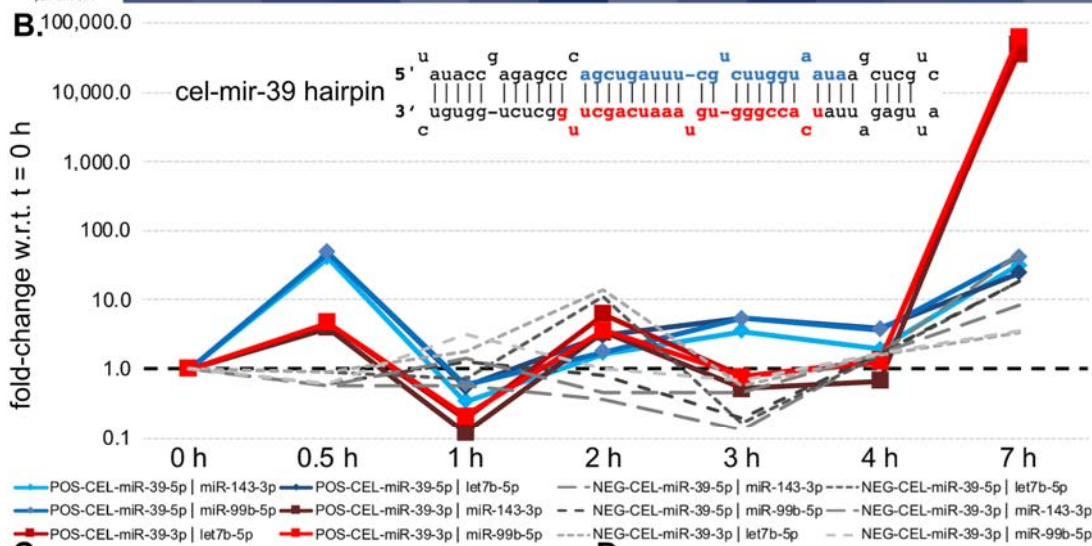
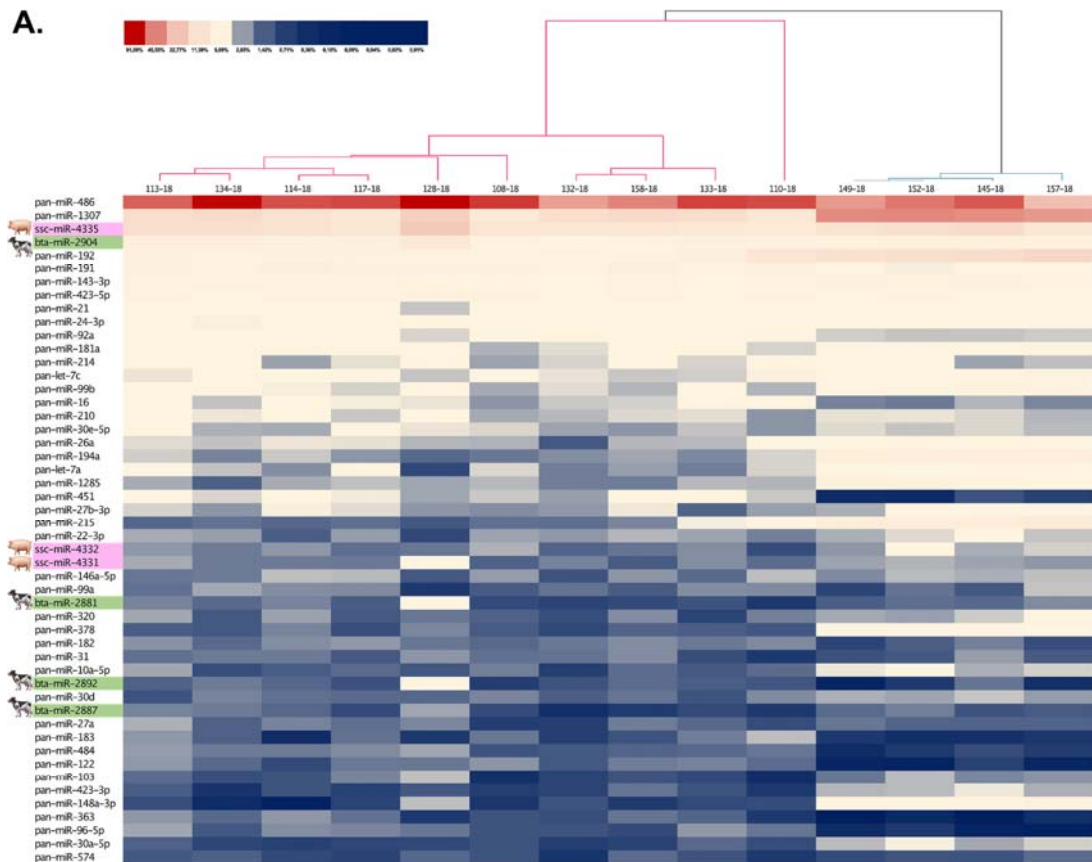


753

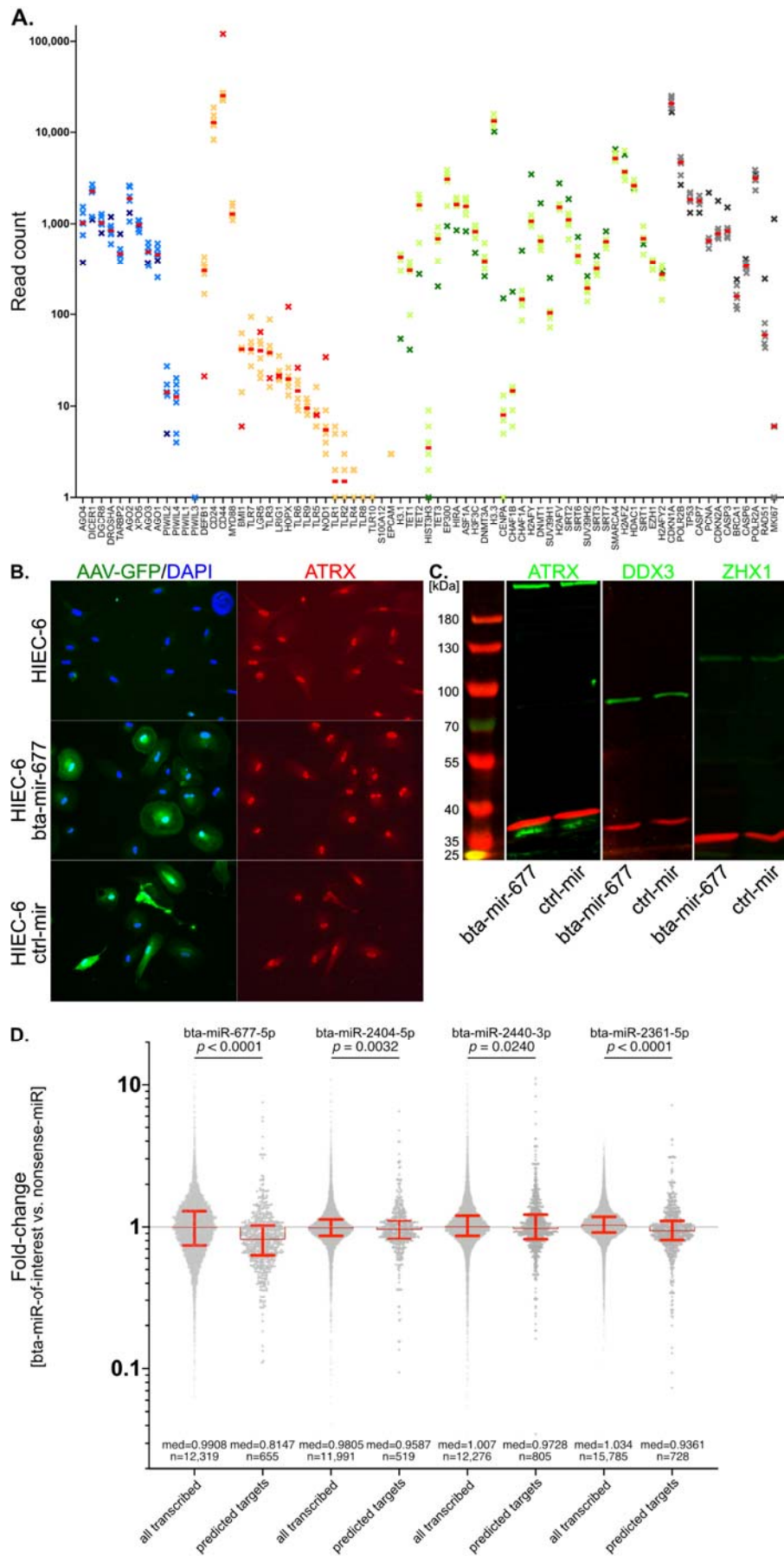
754 **Figure 2.** *Xenobiotic bta-miRs survive the gastrointestinal passage in preterm neonates. A.* Results of

755 qPCR for selected bta-miRs. For comparison, pan-miR-143-3p shared by humans and cattle is shown

756 (red box). The relative enrichment was normalized with respect to pan-miR-99b-5p.



758 **Figure 3.** Reporter *cel-miR-39-3p* accumulates in the bloodstream and *cel-miR-39-5p/-3p* co-
759 precipitate with Argonaute/Ago2 from homogenized intestinal biopsies. **A.** Heat map of miRNAs
760 detected in enriched porcine preterm neonatal intestinal cells following 9 days of enteral bovine
761 colostrum/formula supplementation. Only the top 50 miRNAs found in all species are shown. A
762 colour gradient was used for the visualisation of each miRNA's abundance (read counts per million;
763 CPM) in each specimen. MicroRNAs were sorted in descending order with reference to the median
764 CPM of all specimens. **B.** *C. elegans* (*cel*)-mir-39 hairpin. Prospective guide and passenger strands are
765 highlighted for *cel-miR-39-5p* (blue) and *cel-miR-39-3p* (red). **C.** Results of qPCR. Normalization of
766 *cel-miR-39-5p* and *cel-miR-39-3p* was performed using endogenous pan-miR-143-3p, pan-miR-99b-
767 5p or pan-let-7b-5p, respectively. Blue curves: *cel-miR-39-5p* (POS; *cel-miR-39* feeding); red curves:
768 *cel-miR-39-3p* (POS; *cel-miR-39* feeding); grey curves: (NEG; no *cel-miR-39* supplementation). **D.**
769 Using Chimira [38] for analysis of small RNA sequencing raw data from piglet blood serum miRNAs
770 and selection '*C. elegans*' as species option, we identified *cel-miR-39-3p* (avg. 95 raw read counts).
771 For comparison, matching *cel-let-7-5p* (avg. 2145 raw read counts, sequence identity to *ssc-let-7a-5p*
772 [nt 1-22]) and *cel-miR-72-5p* (avg. 22 raw read counts, probably being identified as *ssc-miR-31-5p*
773 [1nt mismatch]) are shown as well as ambiguous matches for *cel-miR-5592-3p* (avg. 17 raw read
774 counts) and *cel-miR-1818* (avg. 5 raw read counts). Notably, the charts y-axis is DESeq2 normalized
775 read counts. **E.** Results of qPCR after Argonaute pull-down using monoclonal mouse pan-
776 argonaute/Ago2 antibodies (Sigma-Aldrich, MABE56, clone 2A8 [40]) and detection of reporter miRs
777 by qPCR from miRNA libraries prepared from co-precipitated small RNAs.
778
779
780



782 **Figure 4.** Tests for the suppression of predicted human mRNA targets of bta-miR-677 on the protein
783 level for selected candidates and for 4 bta-miRs on the whole transcriptome level. **A.** Mapped raw
784 read counts reflect HIEC-6 gene expression profiles. Selected groups of genes are shown: gene
785 expression related to miRNA biogenesis and RNAi activity (blue asterisks), intestinal epithelial cell
786 markers and innate immunity gene expression (orange asterisks); DNA methylation and chromatin
787 structure related gene expression (green asterisks); cell cycle and proliferation related gene expression
788 (grey asterisk). Untreated HIEC-6 are highlighted in each data column through darker coloured
789 asterisks. Each red line marks the median read count for each data column. **B.** Immunofluorescence
790 microscopy revealed no differences in the nuclear localisation of ATRX upon Ad5-mediated bta-miR-
791 677 gene transfer into primary HIEC-6 cells. ATRX predominantly exhibited nuclear localisation and
792 therein we observed focal accumulations in wt-HIEC-6 as well as in bta-mir-677-treated HIEC-6 and
793 ctrl-mir-treated HIEC-6. We routinely focussed our view to areas wherein cells exhibited GFP-signals
794 of different intensity. This should enable us to detect differences in ATRX distribution, which
795 hypothetically could depend on the level of expressed bta-mir-677. Again, no differences were seen
796 between treated cells and untreated controls. Notably, for PLCXD3 no reliable signals were observed
797 in HIEC-6 cells at all. **C.** When normalized with the GAPDH, no differences in the abundances of
798 ATRX or ZHX1 were observed upon Ad5-mediated bta-miR-677 gene transfer into primary HIEC-6
799 cells in Western analyses, when compared to wild-type (wt) HIEC-6 (not shown) or HIEC-6
800 expressing a control-mir. Using two replicative measurements for quantitative Western Blot analyses
801 via LI-COR Empiria Studio Software, we measured a 24.45% (SD: $\pm 1.68\%$) DDX3 signal reduction
802 in bta-mir-677-treated vs. wt and, respectively, a 37.90% (SD: $\pm 1.90\%$) DDX3 signal reduction in
803 bta-mir-treated vs. ctrl-mir-treated HIEC-6. **D.** Effects of Ad5-mediated expression of 4 selected bta-
804 miRs were studied in HIEC-6 (bta-miR-677-5p; bta-miR-2404-5p; bta-miR-2400-3p; bta-miR-2361-
805 5p) in comparison to HIEC-6 expressing a Ad5-mediated nonsense-miR. Relative fold-changes were
806 compared for the whole HIEC-6 transcriptome and the lists of expressed predicted targets. Predicted
807 targets for each bta-miR comprised of hundreds of mRNAs (i.e. bta-miR-677-5p [n=655]; bta-miR-
808 2404-5p [n=519]; bta-miR-2400-3p [n=805]; bta-miR-2361-5p [n=728]). Statistical power

809 calculations were done using the nonparametric Wilcoxon–Mann–Whitney method and GraphPad
810 Prism 8.4.3 software.

811

812

813 **Supporting information captions**

814 **Figure S1.** *Illustration of theoretical regulatory contributions of breast milk microRNAs in the*
815 *offspring. A.* Posttranscription gene silencing (PTGS) depends on the targeting of mRNAs by
816 microRNAs leading to their suppression through mRNA decay or translational blocking. With respect
817 to any virtual gene-of-interest (GOI) a given microRNA can act directly on a GOIs mRNA or
818 upstream in its regulatory hierarchy on a GOIs master activator’s mRNA or, respectively, on a master
819 repressor mRNA. **B.** The regulatory contribution of breast milk microRNAs can theoretically explain
820 any gene expression pattern observable during and around the nursing period.

821

822 **Figure S2.** *Results of principal component analyses of microRNAs shared by all taxa under*
823 *investigation. Quadrants I and IV (section magnified on the right) harbour all specimens whereby all*
824 *human specimens (blue: hsa1-7) are clustering. Slightly separated is a separated scattered cluster*
825 *harbouring all herbivorous specimens (yellow to green: bta1-4, cae1-2, eas, eca, ogm, ojo) and one*
826 *dog specimen (red arrow: clu). Above is a mini-cluster comprising both porcine specimens (pink:*
827 *ssc1-2) and separated the cat specimen (red: fca).*

828

829 **Figure S3.** *Transduction efficiency.* The efficiency of Ad5-mediated gene transfer to HIEC-6 was
830 measured by flow cytometry. Serial experiments using different MOIs (ctrl, 200, 1000, 5000) in two
831 independent HIEC-6 culture batches (no. 9/10) are shown. Measurements of GFP-positive cells
832 revealed that in HIEC-6 near quantitative transduction (>95% at a $MOI \geq 5.000$) could be achieved 96h
833 post-transduction

834

835 **Figure S4.** *Activity tests for bta-mir-677 using a predicted target sequence cloned into a luciferase 3’-*
836 *UTR gene segment. A.* Cloning of putative bta-miR-677 target motif into the 3’-UTR region of the

837 firefly luciferase gene using SacI and NheI for restriction digest. **B.** Results of firefly luciferase
838 silencing by bta-mir-677-like hairpin RNA co-transfected with pmirGLO (Promega) in HeLa cells.
839 *Renilla* luciferase expression from the same vector was used for normalization in control experiments
840 and upon bta-miR-677-like hairpin co-transfection. Altogether, 22 independent experiments (mock:
841 n=11; bta-miR-677 hairpin: n=11) were conducted.

842

843 **Figure S5.** Tests for the presence of bta-mir-677-like hairpins and mature bta-miR-677-5p or bta-
844 miR-677-3p, respectively. Tests were performed using the Mir-X kit (Takara Bio USA, Inc.) in
845 combination with qPCR and PAGE. **A.** Briefly, poly[A] polymerase was used to tail the 3'-ends of
846 microRNA precursors and mature microRNAs. Subsequently, 5'-adaptor oligo[T]VN was used to
847 prime cDNA synthesis. For qPCR forward primers discriminating precursors and mature microRNAs
848 were used in combination with Mir-X proprietary adaptor-specific reverse primers. **B.** The use of
849 forward primers for mature bta-miR-677-5p (red curves) as well as the bta-mir-677-like hairpin
850 (brownish curves) resulted in reproducible C_T values associated with sharp melting curves in different
851 experiments, whereas the use of primers for mature bta-miR-677-3p resulted in probably unspecific
852 signals (concluded from the irregular melting curves). Control experiments using RNA from wildtype
853 HIEC-6 did not produce reproducible qPCR signals and melting curves (dashed lines in all charts). **C.**
854 The PCR amplicons were separated by PAGE (6% PAA) in order to confirm the predicted size shift
855 between microRNA precursors and mature microRNAs, respectively. The band sizes of the mature
856 bta-miR-677-5p (expected size between 60 and 70 bp) as well as the observed shift with respect to the
857 bta-mir-677-like (hairpin) precursor were in agreement with the theoretical expectations, whereas no
858 specific amplicon could be seen for bta-miR-677-3p and wildtype control experiments.

859

860 **Table S1.** *Differential milk microRNA patterns.* Results of ANOVA analyses for comparative analyses
861 between hominidae vs. bovidae, hominidae vs. suinae, bovidae vs. suinae as well as omnivores vs.
862 herbivores, omnivores vs. carnivores, herbivores vs. carnivores.

863

864 **Table S2.** *Identification of taxon-specific miRNAs.* Comparative overviews and quantification of
865 taxon-specific microRNAs.

866

867 **Table S3.** *Materials' lists.* **A.** List of formula/powdered milk products used in this study. **B.** List of
868 oligonucleotides used in this study

869

870 **Table S4.** *Predicted human mRNA targets for several selected bovine-specific miRNAs.* Results of
871 searches using the custom sequence prediction option of mirDB.org (<http://www.mirdb.org>) for

872 human mRNA target prediction.